Astron. Astrophys. 334, 355–362 (1998)

ASTRONOMY AND ASTROPHYSICS

Twist angles: a method for distinguishing islands, tori and weak chaotic orbits. Comparison with other methods of analysis

Claude Froeschlé[1] **and Elena Lega**[1,2]

[1] Observatoire de la Cote d'Azur CNRS/ UMR 6529 Bd. de l'Observatoire, BP 4229, F-06304 Nice, France
[2] CNRS-LATAPSES, 250 Rue A. Einstein, F-06560 Valbonne, France

Received 1 August 1997 / Accepted 27 January 1998

Abstract. Using the standard map as a model problem we have investigated the method of the twist angles (Contopoulos and Voglis 1997) to distinguish islands tori and weak chaotic orbits. In the case of regular orbits, we have shown the relationship with the frequency studying in particular the case of second order resonances. We have tested the sensitivity of the method comparing it to the frequency analysis, the sup-map analysis and the fast Lyapunov indicator.

Key words: celestial mechanics, dynamical systems – methods: numerical

1. Introduction

The classical method for studying the structure of a dynamical system is that of the Lyapunov Characteristic Exponents (LCEs hereafter, see Benettin et al. 1980 and Froeschlé 1984 for a detailed review). Unfortunately, the computation of the LCEs may take a large amount of time in particular in the case of weak chaos.

Recent theoretical results about the fine structure of a dynamical system (Morbidelli and Giorgilli 1995) as well as numerical results concerning for example the distribution of asteroids (Milani and Nobili 1992) have raised questions which require the systematic exploration of a large number of orbits in order to be answered. Therefore it is very important to develop fast methods of analysis for the study of the structure of a dynamical system.

Two methods have been widely used for Hamiltonian systems: the frequency map analysis (Laskar et al. 1992, Laskar 1993, Lega & Froeschlé 1996) and the sup-map method (Laskar 1990, Froeschlé & Lega 1996). More recently Froeschlé et al. (1997a) have introduced a third method of analysis: the Fast Lyapunov Indicator (FLI hereafter). This method, strictly related to that of the LCEs, is shown to be very sensitive for the detection of weak chaos. Some preliminary applications have been made for studying the structure of the asteroidal belt (Froeschlé et al. 1997b). The FLI is a performant tool for distinguishing between chaotic and regular orbits but it is not able, unlikely the frequency or the sup-map analysis, to distinguish between islands and rotational tori, which are both invariant curves.

With the same purpose of distinguishing chaos from order Contopoulos and Voglis (1997) have introduced an indicator based on the spectra of what they call the "helicity angles". They have shown that this is a fast and sensitive method taking as example a set of orbits belonging either to a chaotic zone or to libration islands.

Using the two-dimensional standard map as a model problem, we show in this paper that this indicator is also able to clearly distinguish between islands and rotational tori (Sect. 2). We then study (Sect. 3) the relation between the frequency and the helicity angles and, in order to have an indication of the sensitivity of the method (Sect. 4), we compare it to the frequency map, the sup-map and the FLI.

2. Definition and application to the two dimensional standard map

Following the general definition given by Contopoulos and Voglis (1997) we define the helicity angle for the particular case of a two dimensional mapping. Lets take the mapping T and the corresponding tangent mapping defined as follows:

$$\begin{cases} \boldsymbol{X}_{n+1} = T\boldsymbol{X}_n \\ \boldsymbol{Y}_{n+1} = (\frac{\partial T}{\partial \boldsymbol{X}_n})\boldsymbol{Y}_n \end{cases} \quad (1)$$

where $\boldsymbol{X}$ and $\boldsymbol{Y}$ belong to $\Re^2$. The helicity angle is the angle ϕ_n formed by the vector $\boldsymbol{Y}_n$ with a fixed direction, say the x-axis. In the case of invariant curves, after a transient regime the image of any initial vector $\boldsymbol{Y}_0$ becomes tangent to the orbit, therefore ϕ measures the deviation of the orbit from a fixed direction.

The distribution of the helicity angles is shown to be invariant in the chaotic domain and depending on initial conditions for invariant orbits (Contopoulos and Voglis 1997). Therefore, the average value $\langle\phi\rangle_N = \sum_{i=1}^{N} \phi_i/N$, after a given number N of iterations, is quite the same for the chaotic domain while changes smoothly for invariant curves. In particular the authors apply their method to distinguish between invariant and chaotic orbits.

Send offprint requests to: C. Froeschlé, (claude@obs-nice.fr)

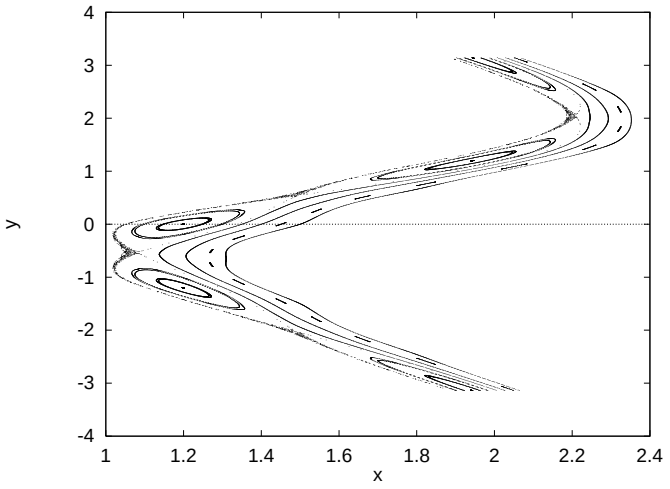

Fig. 1. A set of orbits for the standard map with perturbation parameter $\epsilon = 0.8$.

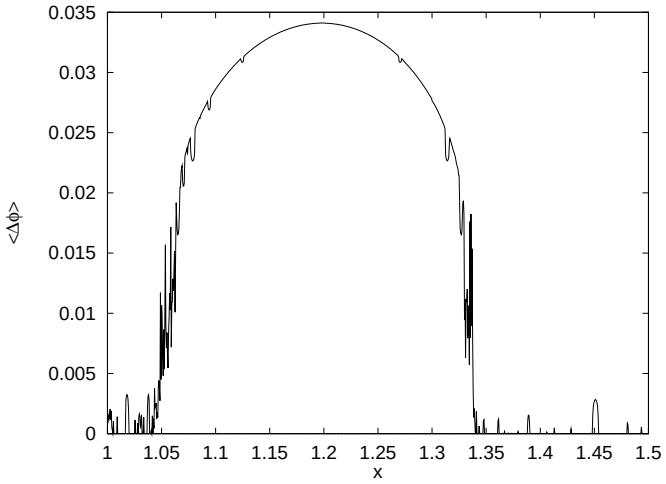

Fig. 2. Variation of the average value of the twist angles computed with 20 000 iterations as a function of the action in the interval $1 < x < 1.5$ for a set of 1 000 orbits of the standard map with $\epsilon = 0.8$.

We consider in the following the "twist angle" $\Delta\phi_n$ (Contopoulos and Voglis 1997) which is equal to the difference of two consecutive helicity angles:

$$\Delta\phi_n = \phi_{n+1} - \phi_n \tag{2}$$

Taking the mean value $\langle\Delta\phi\rangle_N$ we will show that this indicator not only is able to distinguish between invariant and chaotic orbits, but even between islands and tori, which are both invariant curves. For our numerical experiences we have considered as a model problem the standard map (Froeschlé 1970, Lichtenberg & Lieberman 1983):

$$T = \begin{cases} x_{i+1} &= x_i + \epsilon \sin(x_i + y_i) \pmod{2\pi} \\ y_{i+1} &= y_i + x_i \pmod{2\pi} \end{cases} \tag{3}$$

Fig. 1 displays orbits of the standard map of Eq. 3 for $\epsilon = 0.8$. In this figure the usual features of invariant tori appear as well as a chain of islands, corresponding to the 1:4 resonance, surrounded by a small chaotic zone.

For the same interval of actions of the plot, $1 \leq x \leq 1.5$, we have computed, starting at $y = 0$, the average value $\langle\Delta\phi\rangle$ over 20 000 iterations for a set of 1 000 orbits. Fig. 2 shows the variation of $\langle\Delta\phi\rangle$ as a function of x. We can clearly see that all invariant tori have $\langle\Delta\phi\rangle$ equal to zero while a noisy variation of $\langle\Delta\phi\rangle$ corresponds to the small chaotic layer and the "hat-shaped" structures correspond to the crossing of islands.

For all the computations presented in this paper, the angles $\Delta\phi_n$ have been defined in the interval $[-\pi, \pi]$. Since the twist angle is a multi-valued function results could depend on the interval of definition of $\Delta\phi$. A way of avoiding this problem is to verify that the distribution of the twist angles remains inside the interval of definition of $\Delta\phi$. This is the case for the numerical experiments presented in this paper. Results are in agreement with those of Contopoulos and Voglis (1997) and moreover invariant tori are clearly distinguished from islands.

The small "inverse-hat-shaped" structures that we detect inside the 1:4 chain of islands (Fig. 2) are higher order islands. We will explain the significance of this behaviour of $\langle\Delta\phi\rangle$ in the following section.

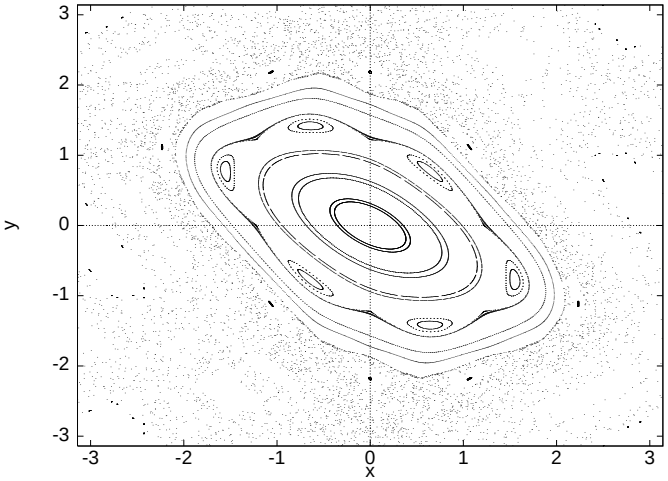

Fig. 3. A set of orbits for the standard map with perturbation parameter $\epsilon = -1.3$.

3. Relationship with the rotation number

It is well known that a fast method for distinguishing the character of a set of orbits is the frequency map analysis (FMA hereafter, Laskar et al. 1992, Laskar 1993). The frequency map is an application which associates to a vector of initial action-like variables the fundamental frequencies of the orbit. The FMA was successfully used in two-dimensional mappings to determine the critical value for which the last invariant torus disappears (Laskar et al. 1992), as well as for the study of global dynamics and diffusion in multi-dimensional systems (Laskar 1993) and for the long time diffusion in particle accelerator dynamics (Dumas & Laskar 1993). More recently it has been used to explore the structure around an invariant KAM torus (Celletti & Froeschlé 1995, Lega & Froeschlé 1996).

In the following, we will consider the standard map for $\epsilon = -1.3$. For this value of the perturbation parameter all invariant tori have disappeared and the largest structure which remains,

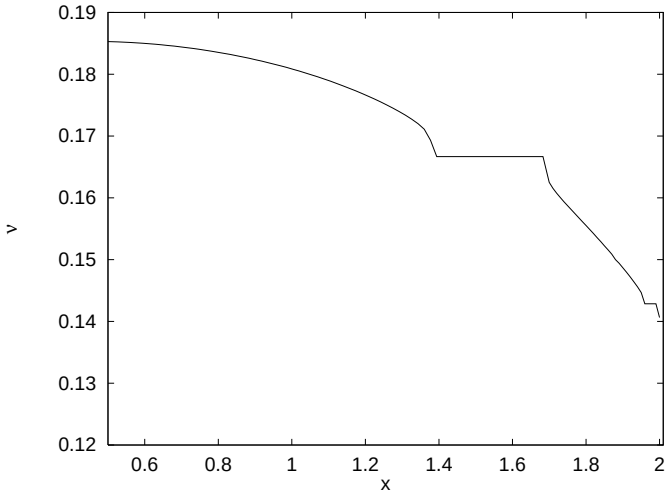

Fig. 4. Variation of the frequency, computed using 20 000 iterations, as a function of the action in the interval $0.5 < x < 2$ for a set of 1 000 orbits of the standard map with $\epsilon = -1.3$.

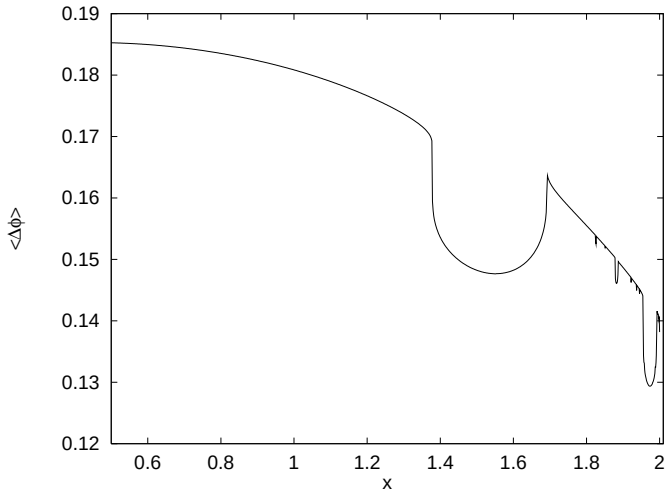

Fig. 5. Same as Fig. 4 for the average value of the twist angles.

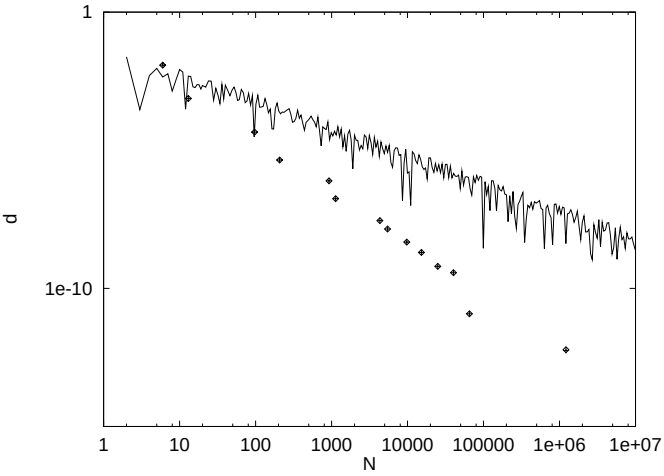

Fig. 6. Variation with the number of iterations N of the difference between the twist angle and the rotation number obtained using 10^7 iterations (continuous line) for an orbit of the standard map with perturbation parameter $\epsilon = -1.3$ and initial conditions $x_0 = 1$, $y_0 = 0$. The two superposed sets of points correspond respectively to the continued fractions expansion of the rotation angle and to the twist angle obtained taking the nearest integer to the sum of $\Delta\phi_i$ over the number of iterations N.

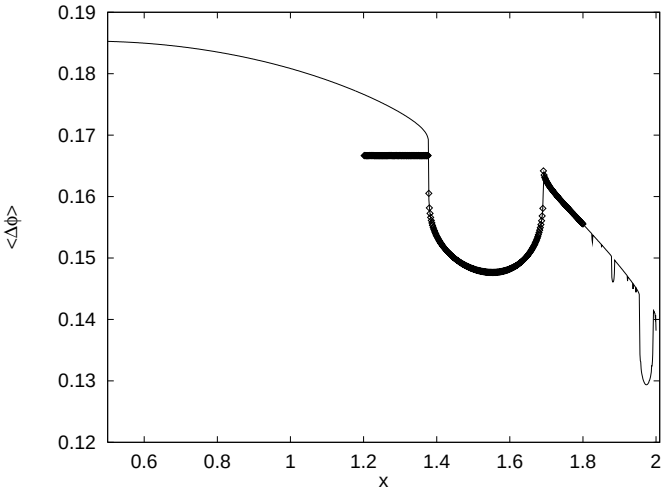

Fig. 7. Variation of the internal frequency $\tilde{\nu}$ of the 1:6 resonance, computed using 20 000 iterations, as a function of the action. In order to compare the internal frequency to the helicity angles we have plotted the sum $1/6+\tilde{\nu}$ (points) as well as the average $\langle\Delta\phi\rangle$ (continuous line).

embedded in a large chaotic sea, is the big island centered on the elliptic point (0,0) (Fig. 3).

We have computed the frequency, or rotation number, using a simplified version of the Hénon's method (the reader can refer to Lega & Froeschlé (1996) for a detailed presentation of the algorithm). Before giving a sketch of the algorithm, let us remark that the rotation number can be defined as the limit when N goes to infinity of the mean of the rotation angles whose definition depends on the topology of the invariant curve. For instance, in the case of an invariant torus the rotation angles are nothing but the differences $\Delta y_i = y_{i+1} - y_i$ and in the case of an island surrounding the origin are the successive angles of rotation around the origin. This is a first method of computation which in fact does not allow to estimate the precision of the computation. Therefore, we have used the following alghoritm. Starting from a point P_0 we iterate N times the mapping and we select the set of successive points P_{n_i} closer to P_0 denoting by n_i their corresponding number of iterations. The rotation number ν is given by:

$$n_i\nu = p_i + \epsilon_i \tag{4}$$

where the integers p_i count the number of revolutions around the invariant curve and the ϵ_i are small quantities which satisfy the inequalities $\epsilon_1 > \epsilon_2 > .....$ The sequence of p_i/n_i appears to be (Lega & Froeschlé 1996) the continued fraction expansion of the rotation number. The relation with the continued fraction expansion ensures that this method of computation gives the best approximation of ν and thanks to the properties of the continued fractions allow us to estimate the precision of the computation.

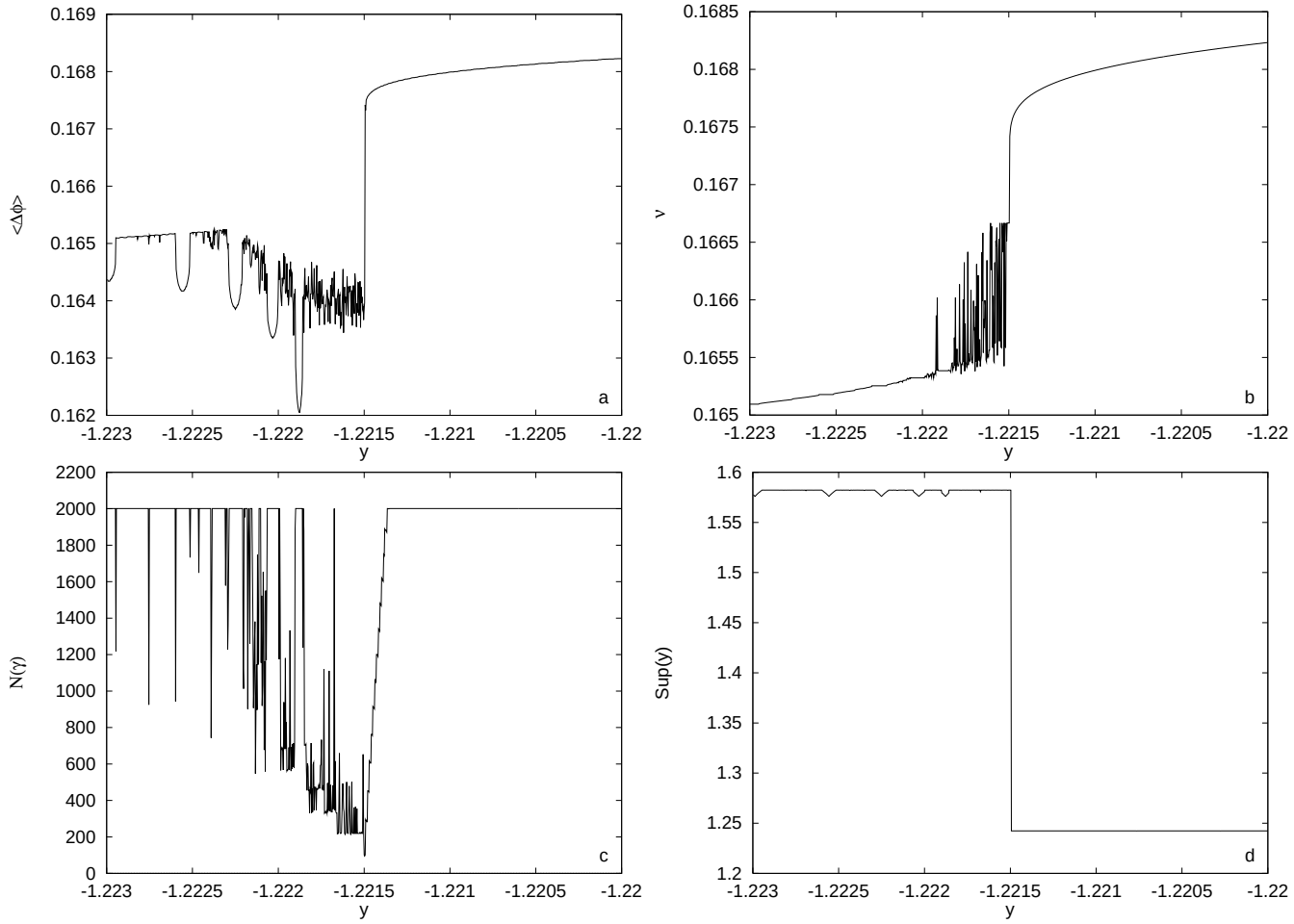

Fig. 8a–d. Cross section for a set of 1 000 orbits in the vicinity of the hyperbolic point associated to the 1/6 resonance of the standard map with perturbation parameter $\epsilon = -1.3$. **a** Average values of the twist angles computed using 20 000 iterations of the mapping. **b** Frequencies of the same set of orbits computed also using 20 000 iterations of the mapping. **c** Number of iterations ($N(\epsilon)$) necessary for the Fast Lyapunov Indicator to reach a threshold value of $\epsilon = 10^{10}$. The maximum number of iterations is $N = 2\,000$. **d** Supremum of y computed using $N = 20\,000$ iterations.

Fig. 4 shows the FMA, computed using $20\,000$ iterations of the mapping, for a set of $1\,000$ orbits with initial conditions on a cross-section of the x-axis, with $0.5 < x < 2$ at $y = -0.75$. The frequency is computed with respect to an observer situated at the origin of the phase space. The monotonic decreasing of the frequency ν up to $x \simeq 1.4$ corresponds to the variation of the speed of rotation around the point $(0, 0)$ of the orbits of the big island. The orbits of the secondary chain of islands (Fig. 3), belonging to the 1:6 resonance, are indicated by the *plateau* at $\nu = 1/6$, from $x \simeq 1.4$ to $x \simeq 1.7$. The smaller *plateau* in Fig. 4 for $x \simeq 1.9$ indicates the presence of an higher order resonance.

Let us remark that for an observer situated in $(0, 0)$, six iterations of the mapping are necessary to make a complete rotation around the origin (and therefore $\nu = 1/6$) for any initial condition on the 1:6 resonance. If we consider an observer in the center of one of the 6 islands and the mapping $T6$ ($Tn = (T \circ T \circ T...)n$ times) the frequency will change monotonically from one initial condition to the other as it is for the previous computation for the central island (Fig. 4). We will call the frequency computed with respect to the center of an island "internal frequency".

We have then computed, for the same set of initial conditions and the same number $N = 20\,000$ of iterations of the mapping the average value of the twist angles $\langle \Delta\phi \rangle_N$. The variation of $\langle \Delta\phi \rangle_N$ (Fig. 5) up to $x \simeq 1.4$ is almost equal to the variation of the frequency. In fact, in this case the frequency of rotation ν around the center $(0, 0)$ is the mean value of the angles formed by the vector $\boldsymbol{X}_{n+1}$ with $\boldsymbol{X}_n$ $\forall n = 1, ...N$ and $\langle \Delta\phi \rangle_N$ is the mean value of the angles formed by the tangent vector $\boldsymbol{Y}_{n+1}$ with $\boldsymbol{Y}_n$, i.e. $\nu \simeq \langle \Delta\phi \rangle_N$ (we would have $\nu \equiv \langle \Delta\phi \rangle_N$ for a pure rotation).

In order to quantify the difference between ν and $\langle \Delta\phi \rangle_N$ we have computed, for an orbit in the central island ($x_0 = 1$, $y_0 = 0$), the difference between the mean value of the twist angles and the rotation number obtained with 10^7 iterations. Fig. 6 shows the convergence of the mean of the twist angles towards the rotation number as a function of N (continuous line). We would have obtained a similar curve for the computation of the

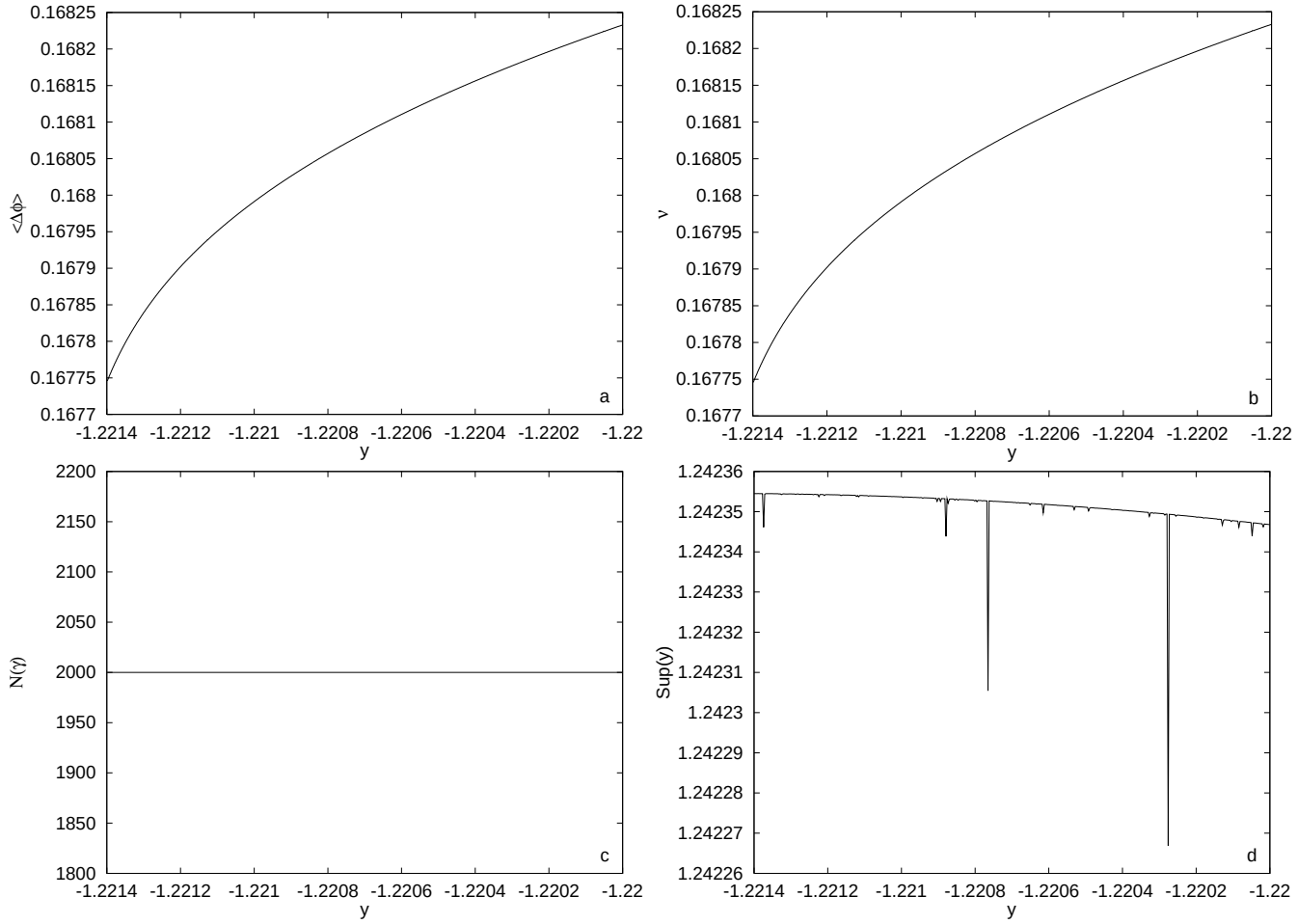

Fig. 9a–d. Same as Fig. 8 for the set of orbits in the interval $-1.2214 \leq y \leq -1.22$, i.e. for orbits in the central island. The monotonic variation of the twist angle (**a**) and of the frequency (**b**) as well as the constancy of $N(\epsilon)$ **c** show that, at this resolution, the whole interval is filled with invariant curves. At this scale it is possible to see the monotonic variation of the supremum of y **d** corresponding to invariant orbits as well as some v-shaped structures which reveal the presence of invariant curves with frequencies very near to rational numbers.

rotation number looking just at the mean of the rotation angles. We have then coupled the computation of the twist angle with the method introduced for the rotation angle, i.e. we have computed $\langle\Delta\phi\rangle_N$ for the successive points P_{n_i} closer to P_0 making a slight modification to the algorithm, i.e. instead of considering just the mean $\sum_{i=1}^{n_i}\langle\Delta\phi\rangle_i/n_i$, we take the nearest integer to the sum of the twist angles. In this case, as shown in Fig. 6 (points) we have obtained exactly the values corresponding to the development in continued fractions of ν. This comes from the fact that the direction of the tangent is more sensitive than the radius vector to the distortion of the curve. We will use in the following this slightly modified definition for $\langle\Delta\phi\rangle$.

Results are different for the crossing of the second order chain of islands. We consider again the 1:6 resonance. The average twist angle, in this case, is not invariant as the frequency is. The computation of $\langle\Delta\phi\rangle_N$ seems to be sensitive to both the rotation around the origin of the phase space and the rotation around the elliptic fixed point of $T6$. In order to test this conjecture we have computed the variation of the internal frequency of the 1:6 resonance.

Starting from an approximated knowledge of the center of one of the six islands we have computed its coordinates (x_c, y_c) solving the equation $\phi(\boldsymbol{x}) = 0$ with $\phi(\boldsymbol{x}) = T6(\boldsymbol{x}) - (\boldsymbol{x})$. Using the simplified version of the Hénon's method sketched at the beginning of this section (Eq. 4) we have computed the frequency $\tilde{\nu}$ with respect to an observer situated in (x_c, y_c). For the computation we have used $20\,000$ iterations of the mapping $T6$. Fig. 7 (points) shows the variation of $\tilde{\nu}$ as a function of x. Outside the "inverse hat shaped" structure corresponding to the island, the flat curve on the left and the decreasing curve on the right are the values of the frequencies obtained for an observer situated in (x_c, y_c). More precisely all the orbits of the left side do not make a complete rotation around the observer and their frequency is therefore zero (the value 1/6 of the figure correspond to a translation of $\tilde{\nu}$ as explained below), while the orbits on the right rotate around the observer with a certain frequency $\tilde{\nu} \neq 0$. In order to compare the internal frequency to the average twist angles we have plotted the sum $1/6 + \tilde{\nu}$ (points) as well as the average $\langle\Delta\phi\rangle$ (continuous line). The exact superposition of the two curves indicates that $\langle\Delta\phi\rangle$, for

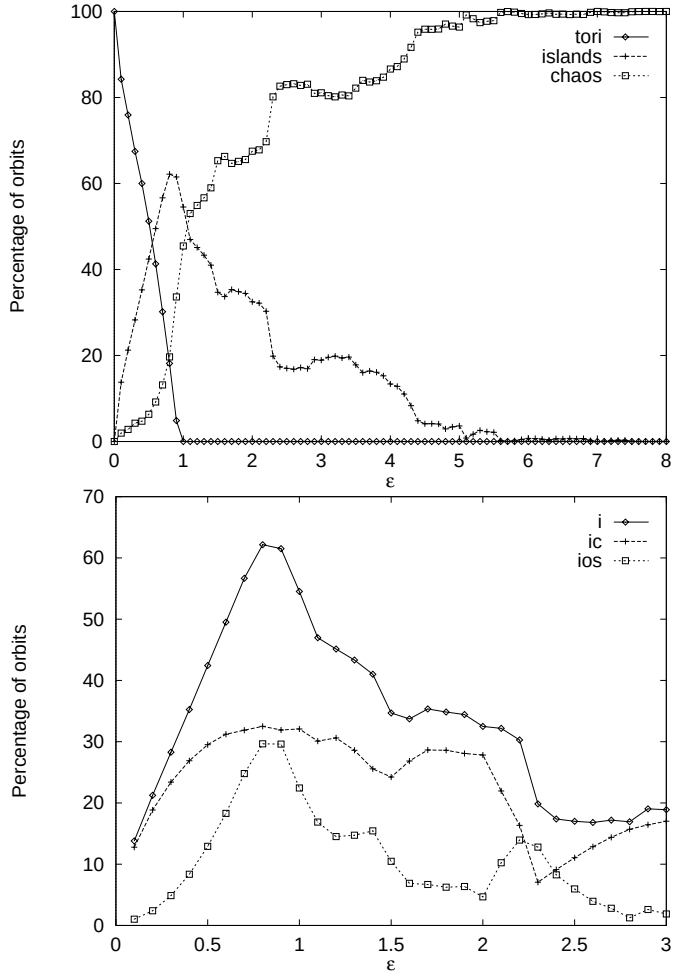

Fig. 10. Percentage of chaotic orbits, invariant tori and libration islands as a function of the perturbation parameter ϵ (top). Percentage of islands as a function of the perturbation parameter ϵ (bottom). The label (i) stands for the whole set of islands, (ic) for the central island, (ios) for the higher order islands.

secondary chain of islands, gives the composition of the rotation around the first order island with the rotation around the center of the secondary order islands. Moreover, the computation of $\langle \Delta\phi \rangle$ gives directly the internal frequency without having to search for the center of the higher order islands.

We remark that in order to use the twist angle as a method for computing the frequency the topology of the curve must be that of a rotation. For instance the average twist angles of the original tori of Fig. 2, which are equal to zero, will give the frequency of rotation under a change in polar coordinates.

4. Comparison and complementarity with other indicators

As we mentioned in the introduction, the reason for the development of new tools of detection of chaos is mainly that of having computational methods faster than the computation of the LCEs, in order to explore large sets of orbits and in particular to detect slow chaotic motion. In fact, as far as strong chaos is concerned, even the LCEs are a fast method of detection.

The problem of detection of slow chaotic layers was already raised by Laskar et al. (1992) who detected chaotic orbits looking at the variation of their frequency with time.

In order to compare the different methods of analysis we have explored the same case than Laskar et al. (1992), i.e., again for the standard map with $\epsilon = -1.3$, the vicinity of an hyperbolic point connected with the 1:6 resonance (Fig. 3). We have computed each indicator for a set of $1\,000$ orbits at $x = 0$ on a cross-section of the y-axis in the interval $-1.223 < y < -1.220$. For one orbit in the vicinity of the hyperbolic point Laskar et al. claim that using the largest LCE: "5×10^6 iterations were necessary to clearly detect the chaotic motion, while it was already visible with the frequency analysis with $20\,000$ iterations".

Fig. 8a shows, for $N = 20\,000$ iterations, the variation of $\langle \Delta\phi \rangle$ and Fig. 8b the variation of the frequency. All the feature appearing in the frequency analysis also appear when looking at the variation of $\langle \Delta\phi \rangle$. We remark that the variation of $\langle \Delta\phi \rangle$ in the interval $-1.2225 \leq y \leq -1.2215$ reveals that, at this resolution, all invariant curves belonging to the big island have disappeared. In fact the values of $\langle \Delta\phi \rangle$ in this interval (Fig. 8a) are all smaller than those obtained in the interval $-1.223 < x < -1.2224$, and, as it is for the frequency, a noisy or non monotonic variation of $\langle \Delta\phi \rangle$ corresponds to the existence of islands or chaotic orbits. It is difficult to obtain the same information with the FMA (Fig. 8b), at least in the interval $-1.2225 < y < -1.2220$, since small noisy variations of the frequency are difficult to separate from a monotonic increasing of the frequency and even from small *plateau*. Moreover, looking at the interval $-1.223 < y < -1.222$ (left side of Fig. 8a) we observe that it is easier to reveal small islands in the case of the helicity angles than in the case of the frequency analysis (the "hat-shaped" structures are easier to see than the *plateau*).

In Fig. 8c we have computed the Fast Lyapunov Indicator (Froeschlé et al. 1997a) for the same set of $1\,000$ orbits. We recall the definition of the FLI for a two-dimensional mapping. Given a two-dimensional basis $\boldsymbol{V}(0) = (v_1(0), v_2(0))$ and an initial condition $P(0) = (x(0), y(0))$ the FLI as a function of the number of iterations n is given by:

$$FLI(n) = \sup_{j=1,2} ||v_j(n)|| \tag{5}$$

The vector $\boldsymbol{V}(n)$ is computed with the tangent mapping of Eq. 1. The idea is that for a chaotic orbit the length of the vector $\boldsymbol{V}(n)$ evolving with the flow increases much faster than for an invariant curve.

In particular in Fig. 8c we have taken as indicator the time $N(\epsilon)$ necessary for the FLI to reach a threshold ϵ with $\epsilon = 10^{10}$. We made the computation over a total number of $N = 2\,000$ iterations. Of course, if the threshold is not reached in less than $2\,000$ iterations we take $N(\epsilon) = N$. All the features appearing in the frequency analysis also appear when looking at the variation of $N(\epsilon)$. We stress the fact that the computation has been made using only $2\,000$ iterations. As we said in the introduction with this method we cannot distinguish between islands and tori.

Finally, we show the variation of the $\sup -y$ computed for the same cross-section taking again $20\,000$ iterations. As shown

by Froeschlé and Lega (1996) the sup-map method is as sensitive as the FMA and it has the advantage of being trivial to compute and therefore to extend to higher dimensional problems. Of course, the sup-map does not carry all the informations contained in the frequency map: for example it clearly detects islands but it does not allows to say to which resonance they belong to.

The v-shaped variations of the $\sup -y$ (Fig. 8d) correspond to islands, the jump stands for the crossing of the hyperbolic point while a monotonic variation reveal the presence of invariant curves. In Fig. 8d the monotonic variations of the $\sup y$ are masked by the amplitude of the jump at the hyperbolic point.

Fig. 9d shows the variation of the sup-map for $1\,000$ orbits in the interval $-1.2214 < y < -1.22$, i.e. for orbits of the central island. The $\sup -y$ decreases monotonically apart for some v-shaped structures which can reveal small islands or orbits with frequencies very near to a rational number (see Contopoulos et al. 1997 for a discussion of this property of the sup-map analysis). In the same interval and at the same resolution, using the other three indicators, $\langle \Delta\phi \rangle$ (Fig. 9a), ν (Fig. 9b) and $N(\epsilon)$ (Fig. 9c), we do not find any small higher order resonance. This indicates that all the $v - shaped$ structures of Fig. 9d are due to a cinematic effect of the sup-y related to the presence of frequencies very near to a rational number.

In our opinion all these methods have to be used as complementary tools.

5. Applications

Using the different tools developed for detecting the dynamical character of the orbits, i.e. the fast Lyapunov indicator to separate chaotic orbits from regular ones and the twist angle to distinguish between original tori and islands, we have computed for different values of the non linearity parameter ϵ the proportions of chaotic orbits, original tori and islands (Fig. 10,top). In order to compute the proportion of chaotic orbits, islands and original tori we have considered a set of 100×100 orbits regularly spaced in the intervals $0 < x < \pi$, $0 < y < \pi$ (for reasons of simmetry this portion of the phase space is a good sample of the whole phase space). The smallest structures detected have therefore a linear size of $\pi/100$. Computing the rotation number we have also separated the contribution of the central island from that of higher order resonances Fig. 10 (bottom).

Fig. 10 (top) shows a quasi linear decrease of the volume occupied by invariant tori which, of course, disappear for a value of ϵ near to one. Up to ϵ of the order of 0.4 the tori are complementary to the big central island whose volume increases linearly with ϵ. For higher values of ϵ higher order resonances become to have a non negligible role (Fig. 10, bottom) and actually when all the original tori disappear we still have a contribution of all islands larger than the chaotic zone. In order to have more than 95% of chaotic orbits we need a value of ϵ greater than 4.5 which shows clearly that the disappearance of invariant tori does not mean a completely chaotic regime.

6. Conclusion

We have numerically investigated the method of the twist angles, introduced by Contopoulos and Voglis (1997), as a tool of detection not only of tori and chaotic orbits but also of islands and secondary islands and of their corresponding frequencies. Actually, as far as frequencies are concerned, the twist angle method is remarkable, not only for its simplicity, but also for its intrinsic character, i.e. for the fact that there is no need to change the center of computation of the rotation angle. This is particularly important because it is not always obvious to define a center as it was already pointed out by Contopoulos (1970). However, difficulties remain which are of the same order that the definition and computation of the rotation angle. The main one is due to the fact that the twist angle (as well as the rotation angle) is a multi-valued function and we have to deal with modulo 2π. For instance when we define the twist angle in the interval $[-\pi, \pi]$ we have problems with orbits whose rotation number is near to π. For it we have proposed to verify that the distribution of the twist angles remain inside the interval of definition.

We have now at our disposal a set of methods to be used all together and which give very precise informations about the character of the orbits as it has been shown when computing the relative proportions of invariant tori chaotic orbits and islands for the two dimensional standard map. Extensions and use for higher dimensions of all these methods are in progress.

References

Benettin G., Galgani L., Giorgilli A., Strelcyn J.M., Lyapunov characteristic exponents for smooth dynamical systems; a method for computing all of them. *Meccanica*, 15:Part I : theory, 9–20 – Part 2 : Numerical applications, –21–30, (1980).

Celletti A., Froeschlé C., On the determination of the stochasticity threshold of invariant curves. *Int. J. of Bif. and Chaos*, 5, n.6:1713–1719, (1995).

Contopoulos G., *Astron. J.*, 75,96.

Contopoulos G., Voglis N., A fast method for distinguishing between order and chaotic orbits. *Astron. Astrophys.*, 317:73, (1997).

Contopoulos G., Voglis N., Efthyomopoulos C., Froeschlé C., Gonczi R., Lega E., Dvorak R., Lohinger E., Transition spectra of dynamical systems. *Celest. Mech. and Dynam. Astron.*, Vol. 67:293–317, (1997).

Dumas H.S., Laskar J., Global dynamics and long-time in Hamiltonian systems via numerical frequency analysis. *Phys. Rev. Lett.*, 70:2975–2979, (1993).

Froeschlé C., A numerical study of the stochasticity of dynamical systems with two degrees of freedom. *Astron. Astrophys.*, 9:15–23, (1970).

Froeschlé C., The Lyapunov characteristic exponents and applications. *Journal de Méc. théor. et apll.*, Numero spécial:101–132, (1984).

Froeschlé C., Gonczi R., Lega E., The fast Lyapunov indicator: a simple tool to detect weak chaos. Application to the structure of the main asteroidal belt. *Planetary and space science*, 45:881–886, (1997b).

Froeschlé C., Lega E., On the measure of the structure around the last KAM torus before and after its break-up. *Celest. Mech. and Dynamical Astron.*, 64:21–31, (1996).

Froeschlé C., Lega E., Gonczi R., Fast Lyapunov indicators. Application to asteroidal motion. *Celest. Mech. and Dynam. Astron.*, 67:41–62, (1997a).

Laskar J., Secular evolution of the Solar system over 10 million years. *Astron. Astrophys.*, 198:341–362, (1988).

Laskar J., The chaotic motion of the Solar system. A numerical estimate of the size of the chaotic zones. *Icarus*, 88:266–291, (1990).

Laskar J., Frequency analysis for multi-dimensional systems. Global dynamics and diffusion. *Physica D*, 67:257–281, (1993).

Laskar J., Froeschlé C., Celletti A., The measure of chaos by the numerical analysis of the fundamental frequencies. Application to the standard mapping. *Physica D*, 56:253, (1992).

Lega E., Froeschlé C., Numerical investigations of the structure around an invariant KAM torus using the frequency map analysis. *Physica D*, 95:97–106, (1996).

Lichtenberg A.J., Lieberman M.A., *Regular and Stochastic motion*. Springer, Berlin, Heidelberg, New York, (1983).

Milani A., Nobili A., An example of stable chaos in the Solar system. *Nature*, 357:569–571, (1992).

Morbidelli A., Giorgilli A., Superexponential stability of KAM tori. *J. Stat. Phys.*, 78:1607-1615, (1995).